Environmental Science and Pollution Research
https://doi.org/10.1007/s11356-020-10908-8

RESEARCH ARTICLE

Ni and TiO_2 nanoparticles cause adhesion and cytoskeletal changes in human osteoblasts

Michal Štefančík[1] · Lucie Válková[1] · Jana Veverková[1] · Jan Balvan[1,2] · Tomáš Vičar[2] · Petr Babula[2] · Josef Mašek[3] · Pavel Kulich[4] · Monika Pávková Goldbergová[1]

Received: 28 May 2020 / Accepted: 16 September 2020

Abstract

Titanium-based alloys have established a crucial role in implantology. As material deteriorates overtime, nanoparticles of TiO_2 and Ni are released. This study is focused on the impact of TiO_2 and Ni nanoparticles with size of 100 nm on cytoskeletal and adhesive changes in human physiological and osteoarthritic osteoblasts. The impact of nanoparticles with concentration of 1.5 ng/mL on actin and tubulin expression and gene expression of FAK and ICAM-1 was studied. The cell size and actin expression of physiological osteoblasts decreased in presence of Ni nanoparticles, while TiO_2 nanoparticles caused increase in cell size and actin expression. Both cell lines expressed more FAK as a response to TiO_2 nanoparticles. ICAM-1 gene was overexpressed in both cell lines as a reaction to both types of nanoparticles. The presented study shows a crucial role of Ni and TiO_2 nanoparticles in human osteoblast cytoskeletal and adhesive changes, especially connected with the osteoarthritic cells.

Keywords Ni nanoparticles · TiO_2 nanoparticles · Osteoblasts · Cytoskeleton · Adhesion · Bone

Background

Alloys based on titanium (nickel-titanium, titanium) have established an important role as biomaterials in medicine over the years, especially in the fields of vascular stent and bone replacement materials. As these materials interact with the human body, there are two forms of interactions described — the leakage of nickel and titanium ions

Highlights
- Osteoblasts incorporate both single nanoparticles and TiO_2 nanoparticle clusters.
- Ni nanoparticles decrease size of physiological osteoblasts and actin expression.
- TiO_2 nanoparticles elongate physiological osteoblasts and increase actin expression.
- Tubulin expression is not affected by Ni and TiO_2 nanoparticles.
- Osteoblasts respond to Ni and TiO_2 nanoparticles via ICAM-1 gene overexpression.

Responsible Editor: Lotfi Aleya

Electronic supplementary material The online version of this article (https://doi.org/10.1007/s11356-020-10908-8) contains supplementary material, which is available to authorized users.

✉ Monika Pávková Goldbergová
goldberg@med.muni.cz

[1] Institute of Pathological Physiology, Faculty of Medicine, Masaryk University, Kamenice 753/5, 625 00 Brno, Czech Republic

[2] Department of Physiology, Faculty of Medicine, Masaryk University, Kamenice 753/5, 625 00 Brno, Czech Republic

[3] Department of Pharmacology and Immunotherapy, Veterinary Research Institute, Hudcova 296/70, 621 00 Brno, Czech Republic

[4] Department of Chemistry and Toxicology, Veterinary Research Institute, Hudcova 296/70, 621 00 Brno, Czech Republic

Published online: 27 September 2020

(Ševčíková et al. 2018; Høl et al. 2019) and release of nanoparticles (Tian et al. 2009) from material degradation, having an impact on cell behavior.

Titanium-based alloys used as vascular stents, joint replacements, or dental implants contain an oxidic layer on their surface composed mostly of TiO_2. This natural amorphous nonstoichiometric layer protects the material from corrosion and degradation (Ferguson et al. 1962; Liu and Thompson 2015). As this layer is degraded, studies have shown that particles of TiO_2 are released into surrounding tissues (Tanaka et al. 2000; Senna et al. 2015). These released particles affect cell metabolism and proliferation in various ways. It was observed that the presence of TiO_2 nanoparticles has a selective impact on cell proliferation with dose-dependent and cell type – dependent influence (Hong et al. 2016; Kukia et al. 2018). Besides TiO_2 nanoparticles released from the oxidic layer, the containment of nickel nanoparticles localized within the TiO_2 layer was described (Tian et al. 2009).

The main mechanism of TiO_2 nanoparticles on cell metabolism is generation of reactive oxygen species within the cell resulting in higher oxidative stress, inflammation, DNA damage, and cell death (Hong et al. 2016; Grande and Tucci 2016). TiO_2 nanoparticles also decrease mitochondrial membrane potential and therefore promote release of cytochrome c into the cytoplasm resulting in cell death (Hong et al. 2016). Similar mechanism of toxicity is observed in Ni nanoparticles — production of reactive oxygen species, DNA damage, and apoptosis induction (Di Bucchianico et al. 2018; Wu and Kong 2020). Besides these mechanisms, Ni nanoparticles induce HIF-1α pathway altering MMP-2 and MMP-9 gene expression (Wan et al. 2011). Malignant transformation potential caused by induction of HIF-1α pathway by Ni nanoparticles was also observed (Pietruska et al. 2011).

Besides nanoparticle release from the surface of titanium-based alloys, nickel and titanium ion release from biomaterial is present. This phenomenon was observed as a direct release of both nickel and titanium ions from stainless steel and NiTi alloys (Azizi et al. 2016; Pettersson et al. 2017; Downarowicz and Mikulewicz 2017; Ševčíková et al. 2018; Mirhashemi et al. 2018; Amanna et al. 2019). As these ions are known for their behavioral effects on cells (viability, proliferation, cell death) and inflammogenic potential (Ali et al. 2016; Zarei et al. 2018), these studies had raised concern in biomaterial safety. Besides direct release from the material, ion release from released nanoparticles was also observed (Mazinanian et al. 2013). Comparing the form of nickel release, it was observed that nanoparticles are rather released than ions (Tian et al. 2009).

Titanium-based alloys used in joint replacement industry also have beneficial effects on the human body, for instance, decreased growth of bacteria and increased growth of osteoblasts (Bhardwaj and Webster 2017); the presented study is focused on degradation products of the alloys on human osteoblasts and human osteoarthritic osteoblasts.

Along with numerous studies on cell proliferation and apoptosis induced by nickel and titanium ions and nanoparticles (Su et al. 2011; Liu et al. 2013; Guo et al. 2015; He et al. 2018), studies also suggest an interaction between nanoparticles and cytoskeletal and adhesion molecules (Zhao et al. 2017; Ghalandari et al. 2019). As these interactions were observed in different types of nanoparticles (silver, gold), our study presents the impact of Ni and TiO_2 nanoparticles on the expression of cytoskeletal proteins — actin and tubulin, and gene expression of adhesive molecules — FAK and ICAM-1.

Methods

The size of TiO_2 and Ni nanoparticles

Titanium(IV) oxide, rutile (637262-100G., St. Louis, USA), and nickel (577995-5G; Sigma-Aldrich Co., St. Louis, USA) were used in this study. To confirm the size of nanoparticles, transmission electron microscopy was used. Samples of TiO2 and Ni nanoparticles were suspended in a drop of distilled water. The resulting suspension was covered with a copper carbon-coated grid (300 Old Mesch, Agar Scientific, Austria). The grid was removed from the suspension after 1 min, and the residual water was dried with a strip of filtration paper. Samples were observed under a transmission electron microscope Philips 208 S Morgagni (FEI, Czech Republic) at accelerating voltage of 80 kV.

Cell culture

In this study, human osteoblasts (Sigma-Aldrich Co., St. Louis, USA) and human osteoblasts-osteoarthritis (Sigma-Aldrich Co., St. Louis, USA) were used. These cell lines provide a reliable model to study nanoparticles' impact on physiological osteoblasts and osteoarthritic osteoblast that had already undergone the inflammatory process as both of the cell lines were isolated from patients.

Both cell lines were cultured in Dulbecco's Modified Eagle's medium/Ham's nutrient mixture F12 (DMEM/F-12, GE Healthcare) and supplemented with 10 mg/mL penicillin/streptomycin (Sigma-Aldrich Co., St. Louis, USA) and 10% fetal bovine serum (FBS, Sigma-Aldrich, St. Louis, USA), under standard growth conditions (37 °C, humidified atmosphere, 5% CO_2/95% O_2 environment). These conditions were maintained throughout the whole study. Cells in the fifth passage were used in this study.

Cells were seeded at a density of 2.0×10^4 cells/cm^2 with the addition of 2.5 mL of medium per dish, and the medium was changed every 2 to 3 days until the required confluence

was reached. Then fresh medium with nanoparticles with a concentration of 1.5 ng/mL of media were added and incubated for 24 h. The concentration of nanoparticles was chosen based on clinical studies of nickel and titanium release from the material after orthopedics surgery. TiO_2 nanoparticle concentration corresponds with serum titanium levels after implantation of cervical disc replacement (Gornet et al. 2017), while Ni nanoparticle concentration correlated with nickel blood levels after total hip arthroplasty (Linden et al. 1985). For control cells, a fresh medium without nanoparticles was added. All experiments were performed with three repeats.

Time-lapse holographic microscopy for cell-metal colocalization

Quantitative phase imaging of living cells was obtained using QPHASE, the coherence-controlled holographic microscope, CCHM (TELIGHT, Brno, Czech Republic). The microscope setup is based on off-axis holography and incorporates a diffraction grating to allow imaging with both spatially and temporally low-coherent illumination. This leads to a high quality of QPI compared with coherent illumination digital holographic microscopy (DHM) by suppressing coherence noise (speckles), interferences, and diffraction artifacts, while the lateral resolution is enhanced closer to a standard light microscope. The off-axis configuration of the system enables a single shot QPI acquisition. Quantitative phase time-lapse imaging was initiated immediately after treating the cells with 1 mg/mL concentration of Ni/TiO_2 nanoparticles. Time-lapse monitoring was performed for 24 h at a frame-rate of 1 frame/3 min. The cells were observed in flow chambers m-Slide I Luer Family Cat. No. 80196 (Ibidi, Martinsried, Germany) in DMEM/F-12 medium for both cell lines. Nikon Plan 10 V/0.3 was used for both holographic observations. Interferograms for holography were taken using a CCD camera (XIMEA MR4021MC). The holographic raw data must be numerically reconstructed. The numerical reconstruction is performed by the custom software where the established methods of the fast Fourier-transform and phase unwrapping are implemented. The output from the software is an unwrapped phase image. This image has intrinsic high contrast and can be processed by an available image processing software.

For the colocalization of BP particles and cells, the novel method based on the merging of phase and amplitude imaging was used. This method combines quantitative phase imaging of weakly scattering or absorbing objects (cells) with the reconstructed amplitude imaging (similar to the bright field microscopy) of amplitude objects (Ni/TiO_2 metal particles) recalculated from the hologram.

Immunofluorescent F-actin staining

After 24 h of incubation with nanoparticles, cells were washed with PBS and fixated with 4% paraformaldehyde for 5 min and then again washed with PBS. For permeabilization, 0.1% Triton-100 X diluted in PBS was used for 5 min, and then cells were again washed with PBS.

For F-actin staining, cells were treated with phalloidin-TRITC (P1951, Sigma-Aldrich) with a concentration of 5 μg/mL of PBS and DAPI (32670-5MG-F, Sigma-Aldrich Co., St. Louis, USA) with the concentration of 0.1 μg/mL of PBS for 40 min. Cells were washed in PBS three times prior to imagining. All steps were carried out under room temperature.

Immunofluorescent tubulin staining

After incubation with nanoparticles was performed, cells were washed with PBS. Then cells were incubated in Tubulin Tracker™ Green 1× (T34075, ThermoFisher Scientific) and 0.01 μg/mL DAPI (32670-5MG-F, Sigma-Aldrich Co., St. Louis, USA) for 30 min in 37 °C incubator. Samples were then washed with PBS three times, fixated with 4% paraformaldehyde, washed in PBS, and examined.

Sample imagining and image analysis

Sample images were taken from random locations using Nikon microscope 20× air objective and NIS Elements software (Nikon) in 8-bit depth (Figs. 1 and 2). Image analysis was held in Zen Blue. According to Vindin et al. (Vindin et al. 2014), cell length and area, nucleus area, and total fluorescence intensity of cells were measured in 20 cells per sample. Relative protein expression was counted as fluorescence intensity: cell area ratio, the nucleus-cytoplasm ratio (NC ratio), was counted as a cell area to the nucleus area ratio. Further data analysis was done using the Mann-Whitney U test in Statistica v. 10.0 (Statsoft Inc., Tulsa, OK) software. The values with $p < 0.05$ were considered significant.

Gene expression analysis

RNA samples were isolated from each sample using TriPure Isolation Reagent (Roche, Basel, Switzerland) according to manufacturers' instruction. Samples' purity was analyzed by measurement of absorbance at wavelengths of 280 nm and 260 nm. Then 260 nm:280 nm ratio was counted. RNA concentration was also measured.

Samples were diluted into 100 ng/mL, and complementary strand synthesis was performed using First Strand cDNA Synthesis Kit (Roche, Basel, Switzerland) according to instructions provided by the manufacturer.

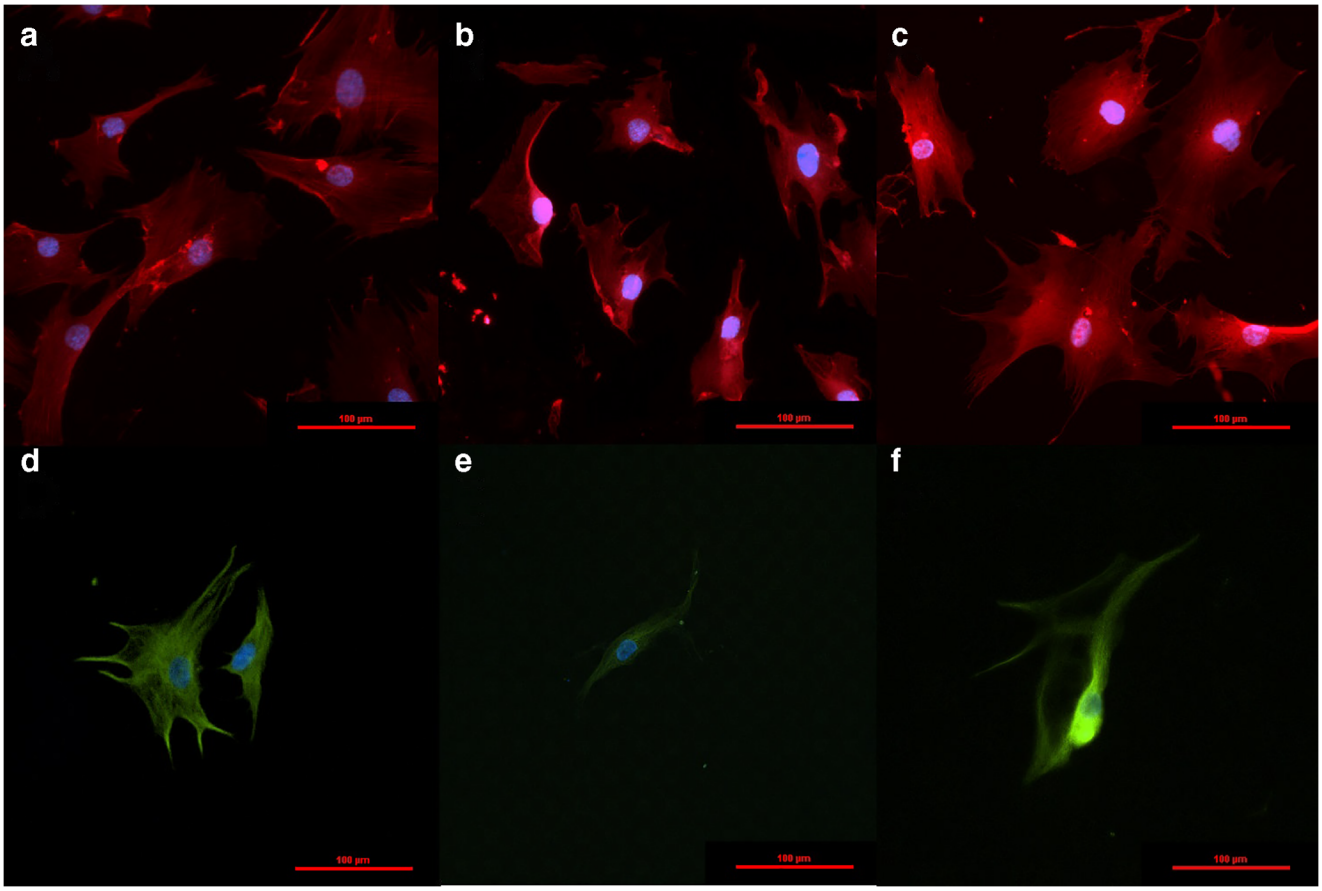

Fig. 1 Fluorescent staining of human physiological osteoblasts. Actin (red): **a** control group, **b** cells with Ni nanoparticles, **c** cells with TiO_2 nanoparticles. Tubulin (green): **d** control group, **e** cells with Ni nanoparticles, **f** cells with TiO_2 nanoparticles; nucleus staining with DAPI, 20× mag, scale bar 100 µm

The final product was used for quantitative PCR with DEPC (RNAse free) water, TaqMan Universal MasterMix no UNG (Applied Biosystems), and TaqMan Gene Expression Assays (Applied Biosystems) in a final reaction volume of 20 µL. Each experiment was performed as a technical triplicate. FAK primer (Hs00178587_m1) and ICAM-1 primer (Hs00164932) and housekeep B2M (4326319E) were used.

Expression data analysis

The expression levels were analyzed via relative expression $2^{-\Delta\Delta Ct}$ method, where $\Delta\Delta CT = [(CT\ target - CT\ housekeep)\ sample - (CT\ target - CT\ housekeep)\ control]$. Values are expressed as median and 5th and 95th percentile. Relative expression > 2 was considered as overexpression of the analyzed gene. Mann-Whitney *U* test was used for the evaluation of mRNA expression levels differences. Statistica v. 10.0 (Statsoft Inc., Tulsa, OK) was used to analyze the data. The values with $p < 0.05$ were considered significant.

Results

The effects of TiO_2 and Ni nanoparticles on cytoskeletal changes in human osteoblasts were observed in this study. To confirm the size of nanoparticles, the nanoparticles were examined using TEM. The size of both TiO_2 and Ni nanoparticles were within the range of 80 to 100 nm (Figs. 3 and 4). The stability of nanoparticles in Dulbecco's Modified Eagle's medium was examined using dynamic light scattering technique. To characterize the number of nanoparticles that were available to interact with cells during the experiment and to shed the possibility that the concentration of free nanoparticles might be lower than expected because a certain fraction was in the form of clusters, the time-lapse holographic microscopy for cell-metal colocalization was performed. The figures from the certain time-lapse (Fig. 5) and the video (supplementary material) showed that the cells incorporate both the nanoparticles of defined size and also the clusters of TiO_2 NP.

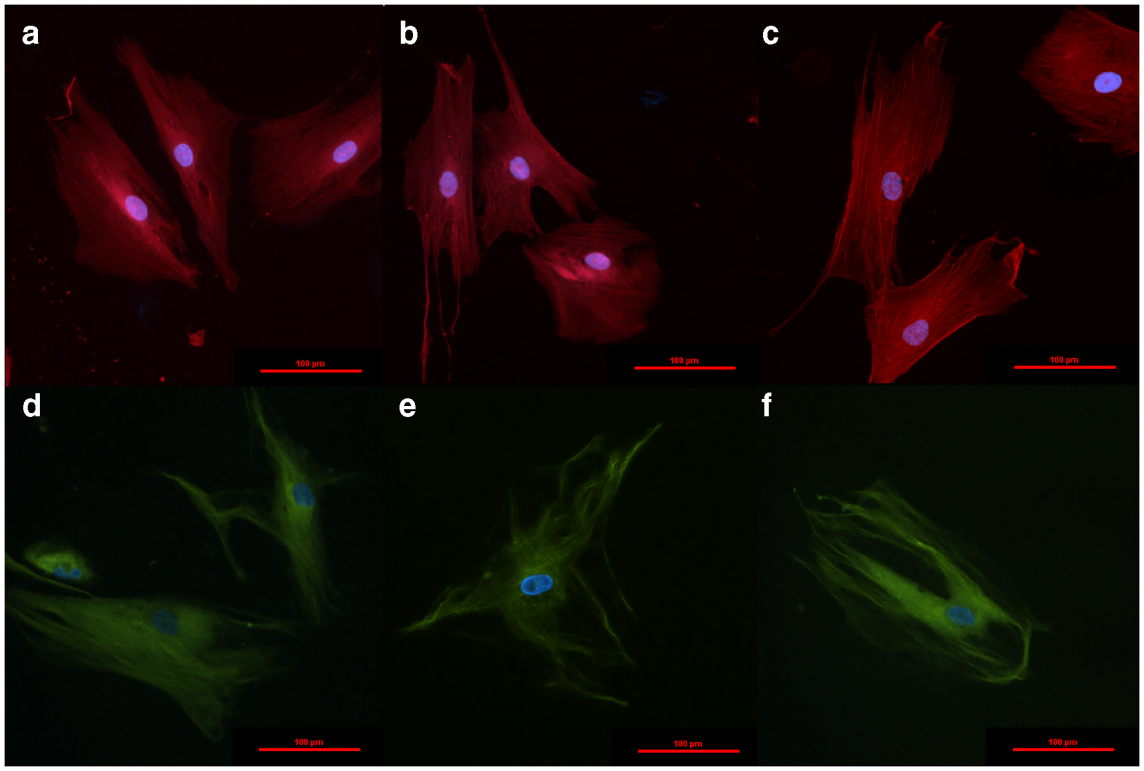

Fig. 2 Fluorescent staining of human osteoarthritic osteoblasts. Actin (red): **a** control group, **b** cells with Ni nanoparticles, **c** cells with TiO_2 nanoparticles. Tubulin (green): **d** control group, **e** cells with Ni nanoparticles, **f** cells with TiO_2 nanoparticles; nucleus staining with DAPI, 20× mag, scale bar 100 μm

The effect of nanoparticles on the size of human physiological osteoblasts

Regarding the cell area and length in physiological osteoblasts, our results summarized in Table 1 (A) showed that nanoparticles caused changes in the size of the cells (Fig. 6). After cultivation with Ni nanoparticles, the cells decreased in size ($p < 0.001$), while TiO_2 nanoparticles led to an increase in the cell size ($p < 0.001$), both compared with control cells. The cell length was also significantly altered. Hand in hand with the size changes, Ni nanoparticles shorten the physiological osteoblasts ($p = 0.001$) and TiO_2 increased the length of the cells ($p = 0.0005$), as presented in Table 1 (B). The nuclei of the cells cultivated with Ni nanoparticles were significantly smaller compared with controls ($p = 0.007$), while no change was observed after cultivation with TiO_2 nanoparticles. Higher nucleus/cell area ratio (NC ratio) was observed in the

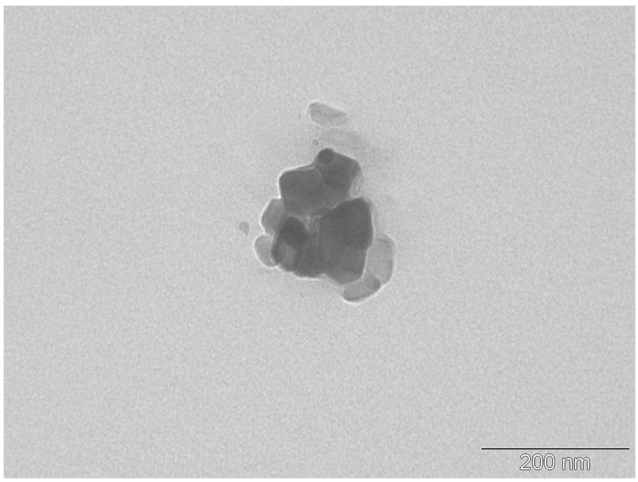

Fig. 3 Transmission electron microscopy of Ni nanoparticles (size < 100 nm); scale bar 200 nm

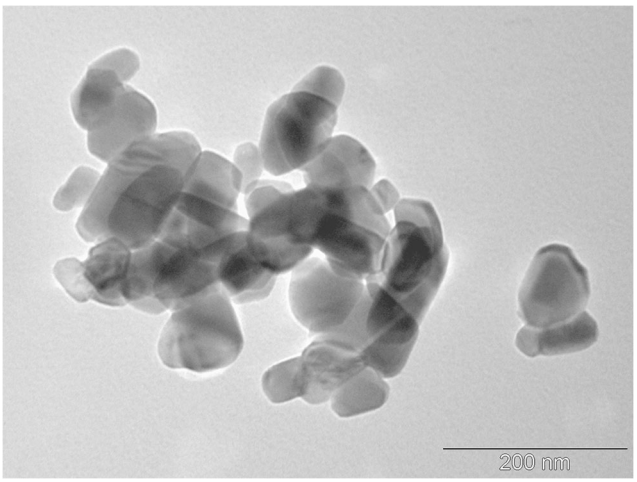

Fig. 4 Transmission electron microscopy of TiO_2 nanoparticles (size < 100 nm); scale bar 200 nm

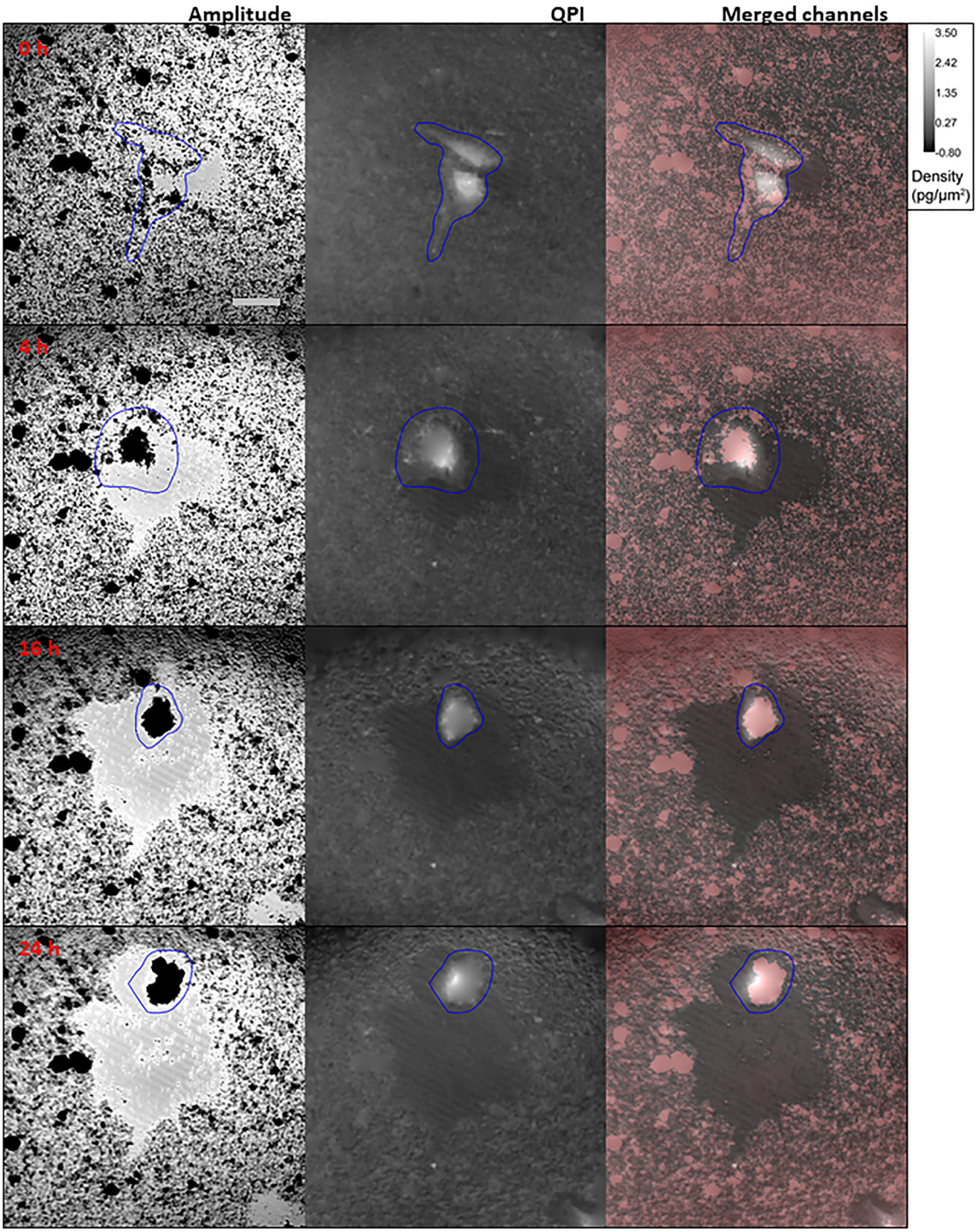

Fig. 5 Colocalization experiment of TiO_2 nanoparticles and human physiological osteoblast cells carried out by merging of phase (middle black images) and amplitude imaging (images in the left column) 0, 4, 16, and 24 h after TiO_2 particles administration. In all images, cells are demarcated by the blue line; TiO_2 nanoparticles are visible as red dots accumulating in the cell through the course of time. In amplitude images (left column), cells are demarcated by the blue line; Ti particles are visible as a black material clustering through the course of time; 10× mag, scale bar 30 μm

presence of Ni nanoparticles ($p = 0.006$), while in the presence of TiO_2 nanoparticles the ratio decreased ($p < 0.001$).

On the other hand, human osteoarthritic osteoblasts were 2-fold larger than physiological osteoblasts ($p < 0.001$), and as a response to Ni and TiO_2 nanoparticles, the cells did not modify the size and the length significantly as shown in Table 1 (A and B). The trend of smaller cell area in the presence of Ni nanoparticles was also observed. Interestingly, the size of

Table 1 Human physiological and osteoarthritic osteoblasts, morphological properties, and cytoskeletal protein expression measurement

			Cell measurement			Actin	Tubulin
(A) Cell type and treatment			Cell area (μm^2)	Cell length (μm)	NC ratio	Total intensity per cell	Total intensity per cell
HOB			7,788.51	135.79	0.044	1,496,429	1,449,232
HOB + NiNP			5,128.27	105.82	0.058	1,139,082	974,403
HOB + TiO_2NP			12,221.29	173.35	0.031	2,591,096	2,285,190
OSBA			14,950.30	194.25	0.022	3,987,351	2,271,647
OSBA + NiNP			11,504.25	179.64	0.024	3,232,491	2,111,698
OSBA + TiO_2NP			15,458.95	192.77	0.023	4,730,134	2,353,746
(B) Cell type	Sample 1	Sample 2	Cell area	Cell length	NC ratio	Total intensity per cell	Total intensity per cell
HOB	Control	NiNP	*< 0.001*	*0.001*	*0.006*	*0.011*	0.121
	Control	TiO_2NP	*< 0.001*	*0.001*	*< 0.001*	*< 0.001*	0.054
	NiNP	TiO_2NP	*< 0.001*	*< 0.001*	*< 0.001*	*< 0.001*	*< 0.001*
OSBA	Control	NiNP	0.116	0.344	0.053	*0.049*	0.571
	Control	TiO_2NP	0.989	0.449	0.310	0.126	0.734
	NiNP	TiO_2NP	0.091	0.072	0.409	*0.007*	0.385

(A) Median values; (B) Mann-Whitney *U* test *p* values of cell measurements — cell area, cell length, nucleus/cytoplasm ratio, and actin and tubulin expression — average intensity per pixel and total intensity per cell measured as the sum of all pixel intensities. Mann-Whitney U test *p* values < 0.05 were considered significant and marked in italics

HOB human physiological osteoblasts, *OSBA* human osteoarthritic osteoblasts, *NiNP* nickel nanoparticles with size 100 nm, *TiO_2NP* titanium dioxide nanoparticles with size 100 nm, *NC ratio* nucleus/cytoplasm ratio

physiological and osteoarthritic osteoblasts after treatment with TiO_2 nanoparticles was similar.

F-actin and tubulin expression changes

As presented in Table 1, the total intensity of the fluorescence of actin fibers was measured (Fig. 6). In both cell lines, Ni nanoparticles caused decreased expression of F-actin protein, in physiological ($p = 0.011$) and osteoarthritic osteoblasts ($p = 0.049$). TiO_2 nanoparticles caused almost 2-fold overexpression of F-actin in physiological osteoblasts ($p < 0.001$) (Table 1 (B)).

According to our results, Ni and TiO_2 nanoparticles did not change the expression of tubulin in human physiological osteoblasts. However, comparing the effect of the nanoparticles, Ni nanoparticles caused a significantly lower expression of tubulin compared with TiO_2 nanoparticles. According to Table 1 (B), there was no significant difference in the expression of tubulin in human osteoarthritic osteoblasts.

Adhesion molecules expression analysis

Relative gene expressions of FAK and ICAM-1 are summarized in Table 2 (A), both compared with control cell culture expression. TiO_2 nanoparticles caused overexpression of FAK gene in both physiological and osteoarthritic cell lines, while Ni nanoparticles caused overexpression of FAK gene only in human physiological osteoblast, with almost no change in osteoarthritic osteoblasts ($p = 0.022$) (Table 2 (B)).

In the case of ICAM-1 gene expression, upregulation of the ICAM-1 gene was observed in all variations, human physiological and osteoarthritic osteoblasts, and cell lines treated with Ni and TiO_2 nanoparticles. Almost 4-fold higher expression of ICAM-1 was observed in osteoarthritic osteoblasts cultivated with Ni nanoparticles compared with physiological cells ($p = 0.005$). Even more, in the case of TiO_2 nanoparticles, a significant more than 5-fold overexpression of ICAM-1 in human osteoarthritic osteoblasts compared with physiological osteoblasts ($p = 0.005$) was observed (Table 2 (B)).

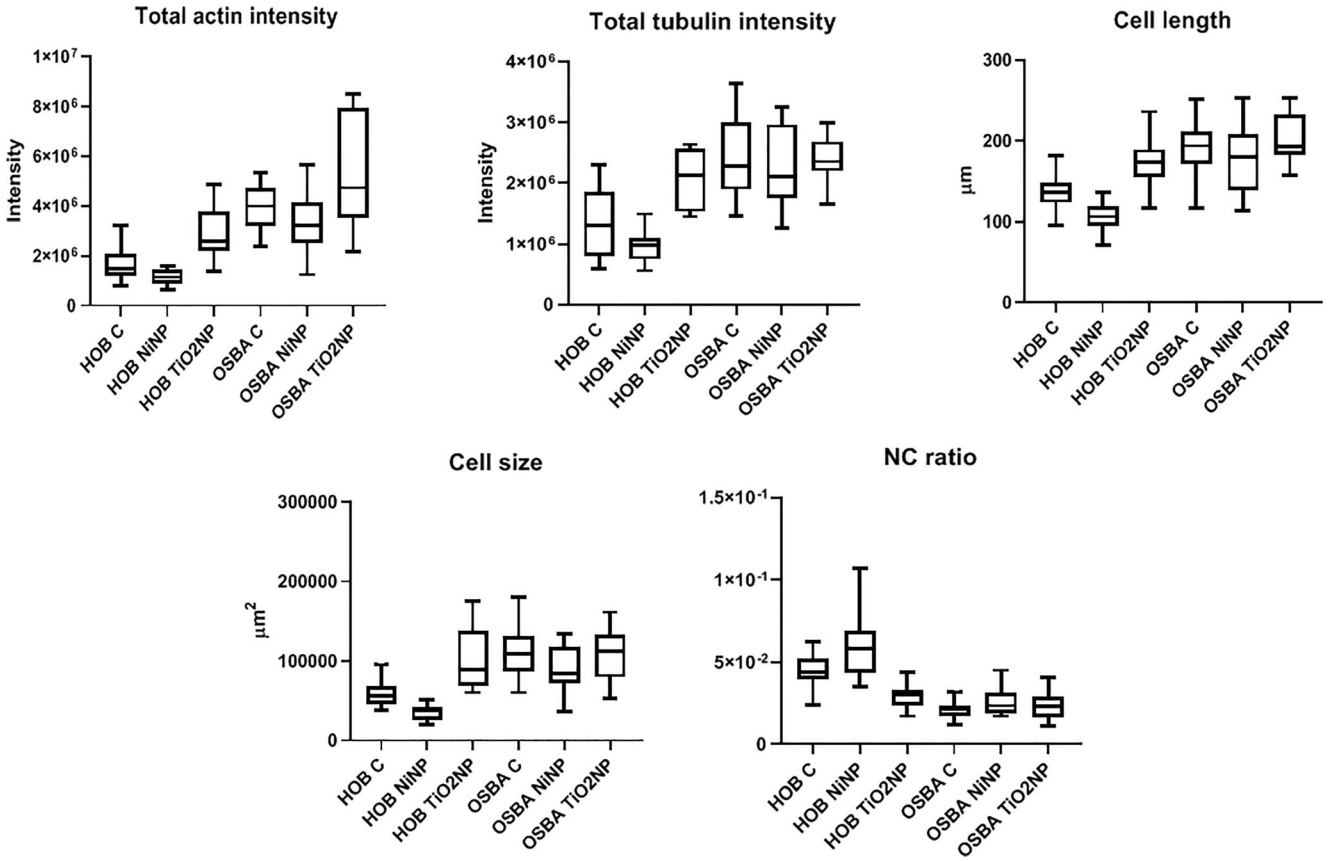

Fig. 6 Comparison between human physiological and osteoarthritic osteoblast with and without the presence of Ni/TiO_2 nanoparticles (total actin and tubulin intensity, cell length, size and NC ratio). HOB human physiological osteoblasts, OSBA human osteoarthritic osteoblasts, C control group without nanoparticles presence, Ni nickel nanoparticles with size 100 nm, TiO_2 titanium dioxide nanoparticles with size 100 nm, NC ratio nucleus/cytoplasm ratio

Table 2 Relative gene expression of FAK and ICAM in human physiological and osteoarthritic osteoblasts after treatment with nanoparticles

(A) Cell type		**Relative gene expression**	
		FAK	**ICAM**
HOB + NiNP		2.38 (1.93; 3.61)	5.15 (1.93; 7.29)
HOB + TiO_2NP		2.21 (1.99; 4.15)	4.36 (2.47; 6.62)
OSBA + NiNP		0.73 (0.49; 2.37)	18.11 (8.53; 32.07)
OSBA + TiO_2NP		2.90 (2.22; 4.83)	26.16 (15.82; 52.10)
(B)			
Sample 1	**Sample 2**	**FAK**	**ICAM**
HOB + NiNP	OSBA + NiNP	*0.022*	*0.005*
HOB + TiO_2NP	OSBA + TiO_2NP	0.230	*0.005*
HOB + NiNP	HOB + TiO_2NP	0.936	0.575
OSBA + NiNP	OSBA + TiO_2NP	*0.035*	0.173

(A) Relative gene expression ($R = 2^{-\Delta\Delta CT}$) of human physiological and osteoarthritic osteoblasts with nanoparticles; median (5th and 95th percentile). (B) Mann-Whitney *U* test *p* values of comparison of relative gene expression ($R = 2^{-\Delta\Delta CT}$) of human physiological and osteoarthritic osteoblasts with nanoparticles. p values < 0.05 were considered significant and marked in italics

FAK focal adhesion kinase (PTK2), *ICAM* intercellular adhesion molecule, *HOB* human physiological osteoblasts, *OSBA* human osteoarthritic osteoblasts, *NiNP* nickel nanoparticles with size 100 nm, *TiO_2NP* titanium dioxide nanoparticles with size 100 nm

Discussion

The impact of nanoparticles has been observed in various cell lines altering their cell proliferation and viability and gene and protein expression. The presented study contributes to further research on the Ni and TiO_2 nanoparticles on human physiological and osteoarthritic osteoblasts related to cytoskeletal and adhesive changes.

Time lapse holographic microscopy

The nanoparticle uptake depends on their size and shape, where smaller and spherical nanoparticles are more likely to be absorbed into cells than nanorods or nanocages (Huerta-García et al. 2019). As nanoparticles cluster into aggregates, they vary in shape and size. Our results suggest that the intake of nanoparticles happens in both forms — single nanoparticles and clusters of nanoparticles. Clusters of nanoparticles are more likely to form in human serum, and their enhanced cellular uptake was observed (Vranic et al. 2017). According to our results, same phenomenon was observed. Moreover, clusters are absorbed by macropinocytosis, which is an active process, involving cytoskeletal changes of actin (Huerta-García et al. 2019), which may lead to actin expression changes caused by TiO_2 nanoparticles presented in our study.

Actin expression alteration

Treatment of cells with Ni nanoparticles in both human physiological and osteoarthritic osteoblasts decreased expression of actin. These findings are supported by the fact that nickel ions, which are released from the Ni nanoparticles, inhibit actin gene expression in vascular smooth muscle cells (Winn et al. 2011). Similar to Ni nanoparticles, silver nanoparticles cause induction on F-actin depolymerization in human skin keratinocytes as well as in human lung and breast adenocarcinoma cells (Zhao et al. 2017), therefore decreased actin protein amount in cells.

In comparison, TiO_2 nanoparticles caused increased actin expression in human physiological osteoblasts. A similar increase of actin expression was observed in cells seeded on titanium samples with TiO_2 nanorods surface assay (Li et al. 2017). Besides actin expression changes, Ibrahim et al. observed the disruption of actin filament orientation caused by TiO_2 nanoparticles with a size of 5 nm and 40 nm (Ibrahim et al. 2018). These reorganization changes may be also connected with the actin-mediated internalization of TiO_2 nanoparticles (Huerta-García et al. 2019).

Considering our results, Ni nanoparticles decrease actin expression and cell size of human physiological and osteoarthritic osteoblasts, while TiO_2 nanoparticles increase the actin expression and cell size of only human physiological osteoblasts.

Tubulin expression changes

Despite our results, that Ni and TiO_2 nanoparticles did not cause any changes in tubulin expression, the microtubule network is a potential target for different types of nanoparticles. Gold nanoparticles bind to tubulin and form complexes, which are used in photo-thermal induction of apoptosis (Ghalandari et al. 2019). Tryptone-stabilized gold nanoparticles reduce cell viability and induce apoptosis via binding to tubulin and promote its acetylation, causing cell cycle arrest and eventually programmed cell death (Mahaddalkar et al. 2017). Another example of tubulin nanoparticle interaction is the fact that cerium oxide nanoparticles bind to tubulin and cause inhibition of differentiation of neural stem cells (Gliga et al. 2017).

Expression of FAK and ICAM-1

Our results proved that TiO_2 nanoparticles cause an increase of FAK gene in both human physiological and osteoarthritic osteoblasts. However, studies of preosteoblasts grown on TiO_2 nanotubes contemplated the downregulated FAK gene expression (Zhang et al. 2015). These finding suggests the difference between TiO_2 nanotubes and TiO_2 nanoparticles on FAK gene expression. On the contrary, silicon-doped TiO_2 film, as a form of material modification, caused overexpression of FAK gene in osteoblast-like cells, suggesting that different surface modification cause different FAK gene expression (Wang et al. 2013).

Considering our results, cell area alteration presented in Table 1 may be explained by the changes of cytoskeletal actin alignment caused by nanoparticles (Cabezas et al. 2019). Therefore, increased cell size and dysregulation of cytoskeletal stability may result in increased FAK expression, as more adhesive proteins may be required to stabilize the instability. Moreover, increased FAK expression may be also supported by the fact that FAK protein pays a crucial role in cell motility and elongation (Katoh 2020), both observed in this study caused by TiO_2 nanoparticles. The variety of changes in FAK expression caused by Ni nanoparticles may be linked to Ni-mediated caspase activation as cells may already start the apoptotic process (Li and Zhong 2014).

A study by Lavigne et al. divides osteoblasts into the population of low and high ICAM-1 expressing cells. High-expressing osteoblasts are the major population of osteoblasts in osteoarthritic and osteoporotic patients (Lavigne et al. 2004). In our case, the basal expression of ICAM-1 by the control cells in both lines was on the same level. Although the ICAM-1 expression of the cells cultivated with Ni and TiO_2 nanoparticles was increased, the major impact of the metal nanoparticles was visible in osteoarthritic osteoblasts. This overexpression can be associated with increased adherence of monocytes and osteoblasts precursors and is associated with increased

production of osteoclast differentiation factor (Tanaka et al. 2000). The interconnection between osteoarthritic cells and the inflammatory cells may be explained by the previous contact with inflammation, suggesting possible existence of "inflammatory preconditioning" (Válková et al. 2018). This impact on osteoclasts may be a partial explanation to the process of loosening of joint replacement, as after surgery, many nanoparticles are released from the material as a result of mechanical implantation, nanoparticles are also a part of bone cement, and more nanoparticles are released from the material over time.

The overexpression of ICAM-1 gene caused by Ni nanoparticles was observed in both physiological and osteoarthritic osteoblasts. On the contrary, human dermal microvascular endothelial cells incubated with significantly higher concentration of Ni nanoparticles did not express more ICAM-1 (Peters et al. 2007). Considering that Ni nanoparticles can release of Ni ions from their surface (Hahn et al. 2012) and Ni ions can cause an overexpression of ICAM-1 in different cell lines (Cortijo et al. 2010; Tsou et al. 2013), this may be the mechanism causing overexpression of ICAM-1 in osteoblasts. Furthermore, our findings contribute to cell type–dependent and concentration-dependent effects approach of nanoparticles.

In conclusion, Ni and TiO_2 nanoparticles released from joint replacement materials play a crucial role in the actin filament dynamics of human physiological and osteoarthritic osteoblasts. Ni nanoparticles cause decreased size of physiological osteoblasts and actin expression, while TiO_2 nanoparticles are responsible for the enlargement of physiological osteoblasts and increased actin expression. The increased expression of actin may be explained by actin-mediated incorporation of nanoparticles into the cells as presented in previous studies (Huerta-García et al. 2019). This process can lead to increase cells size, as our time-lapse suggests chemotactic effect of nanoparticles, which is not dependent on size, as both nanoparticles and clusters are incorporated. However, tubulin expression is not affected by these types of nanoparticles. Increased expression of the ICAM-1 gene was observed as a response to nanoparticles, likely playing one of the major roles in the mechanism of loosening of joint replacement via osteoclast stimulation pathway.

Author contributions All authors contributed to the study conception and design. Material preparation, data collection, and methodology were performed by Michal Štefančík, Lucie Válková, Jana Veverková, Josef Mašek, Pavel Kulich, and Jan Balvan. Analysis were performed by Tomáš Vičar and Monika Pávková Goldbergová. The first draft of the manuscript was written by Michal Štefančík and Monika Pávková Goldbergová, and all authors commented on previous versions of the manuscript. All authors read and approved the final manuscript.

Funding This study was funded by The Ministry of Health Foundation under the contract no. NU20-08-00149, Masaryk University grant (MUNI/A/1453/2019), Institutional Research Concept MZE-RO0518, and The Ministry of Education, Youth and Sports project FIT No. CZ.02.1.01/0.0/0.0/15_003/0000495.

Data availability The datasets used and/or analyzed during the current study are available from the corresponding author on reasonable request.

Compliance with ethical standards

Conflict of interest The authors declare that they have no conflict of interest.

Ethical approval Not applicable

Consent to participate Not applicable

Consent to publish Not applicable

References

Ali A, Suhail M, Mathew S, Shah MA, Harakeh SM, Ahmad S, Kazmi Z, Rahman Alhamdan MA, Chaudhary A, Damanhouri GA, Qadri I (2016) Nanomaterial induced immune responses and cytotoxicity. J Nanosci Nanotechnol 16:40–57

Amanna EN, Bhat SS, Hegde SK (2019) An in vitro evaluation of nickel and chromium release from different commercially available stainless steel crowns. J Indian Soc Pedodontics Prev Dent 37:31–38. https://doi.org/10.4103/JISPPD.JISPPD_176_17

Azizi A, Jamilian A, Nucci F, Kamali Z, Hosseinikhoo N, Perillo L (2016) Release of metal ions from round and rectangular NiTi wires. Prog Orthod 17:10. https://doi.org/10.1186/s40510-016-0123-3

Bhardwaj G, Webster TJ (2017) Reduced bacterial growth and increased osteoblast proliferation on titanium with a nanophase TiO2 surface treatment. Int J Nanomedicine 12:363–369. https://doi.org/10.2147/IJN.S116105

Cabezas MD, Meckes B, Mirkin CA, Mrksich M (2019) Subcellular control over focal adhesion anisotropy, independent of cell morphology, dictates stem cell fate. ACS Nano 13:11144–11152. https://doi.org/10.1021/acsnano.9b03937

Cortijo J, Milara J, Mata M, Donet E, Gavara N, Peel SE, Hall IP, Morcillo EJ (2010) Nickel induces intracellular calcium mobilization and pathophysiological responses in human cultured airway epithelial cells. Chem Biol Interact 183:25–33. https://doi.org/10.1016/j.cbi.2009.09.011

Di Bucchianico S, Gliga AR, Åkerlund E et al (2018) Calcium-dependent cyto- and genotoxicity of nickel metal and nickel oxide nanoparticles in human lung cells. Part Fibre Toxicol 15:32. https://doi.org/10.1186/s12989-018-0268-y

Downarowicz P, Mikulewicz M (2017) Trace metal ions release from fixed orthodontic appliances and DNA damage in oral mucosa cells by in vivo studies: a literature review. Adv Clin Exp Med 26:1155–1162. https://doi.org/10.17219/acem/65726

Ferguson ABJ, Akahoshi Y, Laing PG, Hodge ES (1962) Trace metal ion concentration in the liver, kidney, spleen, and lung of normal rabbits. JBJS 44:317–322

Ghalandari B, Asadollahi K, Shakerizadeh A, Komeili A, Riazi G, Kamrava SK, Attaran N (2019) Microtubule network as a potential candidate for targeting by gold nanoparticle-assisted photothermal therapy. J Photochem Photobiol B Biol 192:131–140. https://doi.org/10.1016/j.jphotobiol.2019.01.012

Gliga AR, Edoff K, Caputo F, Källman T, Blom H, Karlsson HL, Ghibelli L, Traversa E, Ceccatelli S, Fadeel B (2017) Cerium oxide nanoparticles inhibit differentiation of neural stem cells. Sci Rep 7:9284. https://doi.org/10.1038/s41598-017-09430-8

Gornet MF, Singh V, Schranck FW, Skipor AK, Jacobs JJ (2017) Serum metal concentrations in patients with titanium ceramic composite

cervical disc replacements. Spine 42:366–371. https://doi.org/10.1097/BRS.0000000000001745

Grande F, Tucci P (2016) Titanium dioxide nanoparticles: a risk for human health? Mini-Rev Med Chem. https://www.eurekaselect.com/140530/article. Accessed 20 Aug 2020

Guo H, Chen L, Cui H, Peng X, Fang J, Zuo Z, Deng J, Wang X, Wu B (2015) Research advances on pathways of nickel-induced apoptosis. Int J Mol Sci 17. https://doi.org/10.3390/ijms17010010

Hahn A, Fuhlrott J, Loos A, Barcikowski S (2012) Cytotoxicity and ion release of alloy nanoparticles. J Nanopart Res 14:1–10. https://doi.org/10.1007/s11051-011-0686-3

He X-B, Ma T, Zheng W et al (2018) Nano-sized titanium alloy particles inhibit the proliferation and promote the apoptosis of bone marrow mesenchymal stem cells in vitro. Mol Med Rep 17:2271–2276. https://doi.org/10.3892/mmr.2017.8105

Høl PJ, Gjerdet NR, Jonung T (2019) Corrosion and metal release from overlapping arterial stents under mechanical and electrochemical stress – an experimental study. J Mech Behav Biomed Mater 93:31–35. https://doi.org/10.1016/j.jmbbm.2019.02.001

Hong F, Zhao X, Chen M, Zhou Y, Ze Y, Wang L, Wang Y, Ge Y, Zhang Q, Ye L (2016) TiO2 nanoparticles-induced apoptosis of primary cultured Sertoli cells of mice. J Biomed Mater Res A 104:124–135. https://doi.org/10.1002/jbm.a.35548

Huerta-García E, Ramos-Godinez MDP, López-Saavedra A et al (2019) Internalization of titanium dioxide nanoparticles is mediated by actin-dependent reorganization and clathrin- and dynamin-mediated endocytosis in H9c2 rat cardiomyoblasts. Chem Res Toxicol 32:578–588. https://doi.org/10.1021/acs.chemrestox.8b00284

Ibrahim M, Schoelermann J, Mustafa K, Cimpan MR (2018) TiO2 nanoparticles disrupt cell adhesion and the architecture of cytoskeletal networks of human osteoblast-like cells in a size dependent manner. J Biomed Mater Res A 106:2582–2593. https://doi.org/10.1002/jbm.a.36448

Katoh K (2020) FAK-dependent cell motility and cell elongation. Cells 9:192. https://doi.org/10.3390/cells9010192

Kukia NR, Rasmi Y, Abbasi A et al (2018) Bio-effects of TiO2 nanoparticles on human colorectal cancer and umbilical vein endothelial cell lines. Asian Pac J Cancer Prev 19:2821–2829. https://doi.org/10.22034/APJCP.2018.19.10.2821

Lavigne P, Benderdour M, Lajeunesse D, Shi Q, Fernandes JC (2004) Expression of ICAM-1 by osteoblasts in healthy individuals and in patients suffering from osteoarthritis and osteoporosis. Bone 35:463–470. https://doi.org/10.1016/j.bone.2003.12.030

Li Z, Qiu J, Du LQ et al (2017) TiO2 nanorod arrays modified Ti substrates promote the adhesion, proliferation and osteogenic differentiation of human periodontal ligament stem cells. Mater Sci Eng C 76:684–691. https://doi.org/10.1016/j.msec.2017.03.148

Li X, Zhong F (2014) Nickel induces interleukin-1β secretion via the NLRP3-ASC-caspase-1 pathway. Inflammation 37:457–466. https://doi.org/10.1007/s10753-013-9759-z

Linden JV, Hopfer SM, Gossling HR, Sunderman FW (1985) Blood nickel concentrations in patients with stainless-steel hip prostheses. Ann Clin Lab Sci 15:459–464

Liu Z, Thompson GE (2015) Formation of porous anodic oxide film on titanium in phosphoric acid electrolyte. J Mater Eng Perform 24:59–66. https://doi.org/10.1007/s11665-014-1262-7

Liu C-M, Zheng G-H, Ming Q-L, Chao C, Sun JM (2013) Sesamin protects mouse liver against nickel-induced oxidative DNA damage and apoptosis by the PI3K-Akt pathway. J Agric Food Chem 61:1146–1154. https://doi.org/10.1021/jf304562b

Mahaddalkar T, Mehta S, Cheriyamundath S, Muthurajan H, Lopus M (2017) Tryptone-stabilized gold nanoparticles target tubulin and inhibit cell viability by inducing an unusual form of cell cycle arrest. Exp Cell Res 360:163–170. https://doi.org/10.1016/j.yexcr.2017.09.002

Mazinanian N, Hedberg Y, Odnevall Wallinder I (2013) Nickel release and surface characteristics of fine powders of nickel metal and nickel oxide in media of relevance for inhalation and dermal contact. Regul Toxicol Pharmacol 65:135–146. https://doi.org/10.1016/j.yrtph.2012.10.014

Mirhashemi A, Jahangiri S, Kharrazifard M (2018) Release of nickel and chromium ions from orthodontic wires following the use of teeth whitening mouthwashes. Prog Orthod 19:4. https://doi.org/10.1186/s40510-018-0203-7

Peters K, Unger RE, Gatti AM, Sabbioni E, Tsaryk R, Kirkpatrick CJ (2007) Metallic nanoparticles exhibit paradoxical effects on oxidative stress and pro-inflammatory response in endothelial cells in vitro. Int J Immunopathol Pharmacol 20:685–695. https://doi.org/10.1177/039463200702000404

Pettersson M, Kelk P, Belibasakis GN, Bylund D, Molin Thorén M, Johansson A (2017) Titanium ions form particles that activate and execute interleukin-1β release from lipopolysaccharide-primed macrophages. J Periodontal Res 52:21–32. https://doi.org/10.1111/jre.12364

Pietruska JR, Liu X, Smith A, McNeil K, Weston P, Zhitkovich A, Hurt R, Kane AB (2011) Bioavailability, intracellular mobilization of nickel, and HIF-1α activation in human lung epithelial cells exposed to metallic nickel and nickel oxide nanoparticles. Toxicol Sci 124:138–148. https://doi.org/10.1093/toxsci/kfr206

Senna P, Del Bel Cury AA, Kates S, Meirelles L (2015) Surface damage on dental implants with release of loose particles after insertion into bone. Clin Implant Dent Relat Res 17:681–692. https://doi.org/10.1111/cid.12167

Ševčíková J, Bártková D, Goldbergová M, Kuběnová M, Čermák J, Frenzel J, Weiser A, Dlouhý A (2018) On the Ni-ion release rate from surfaces of binary NiTi shape memory alloys. Appl Surf Sci 427:434–443. https://doi.org/10.1016/j.apsusc.2017.08.235

Su L, Deng Y, Zhang Y, Li C, Zhang R, Sun Y, Zhang K, Li J, Yao S (2011) Protective effects of grape seed procyanidin extract against nickel sulfate-induced apoptosis and oxidative stress in rat testes. Toxicol Mech Methods 21:487–494. https://doi.org/10.3109/15376516.2011.556156

Tanaka N, Ichinose S, Kimijima Y, Mimura M (2000) Investigation of titanium leak to bone tissue surrounding dental titanium implant: electron microscopic findings and analysis by electron diffraction. Med Electron Microsc 33:96–101. https://doi.org/10.1007/s007950000016

Tanaka Y, Maruo A, Fujii K, Nomi M, Nakamura T, Eto S, Minami Y (2000) Intercellular adhesion molecule 1 discriminates functionally different populations of human osteoblasts: characteristic involvement of cell cycle regulators. J Bone Miner Res 15:1912–1923. https://doi.org/10.1359/jbmr.2000.15.10.1912

Tian H, Schryvers D, Shabalovskaya S, Humbeeck JV (2009) TEM study of the mechanism of Ni ion release from Nitinol wires with original oxides. In: European Symposium on Martensitic Transformations. EDP Sci 05027

Tsou T-C, Liou S-H, Yeh S-C, Tsai FY, Chao HR (2013) Crucial role of Toll-like receptors in the zinc/nickel-induced inflammatory response in vascular endothelial cells. Toxicol Appl Pharmacol 273:492–499. https://doi.org/10.1016/j.taap.2013.09.014

Válková L, Ševčíková J, Pávková Goldbergová M, Weiser A, Dlouhý A (2018) Osteoarthritic process modifies expression response to NiTi alloy presence. J Mater Sci Mater Med 29:146. https://doi.org/10.1007/s10856-018-6156-z

Vindin H, Bischof L, Gunning P, Stehn J (2014) Validation of an algorithm to quantify changes in actin cytoskeletal organization. J Biomol Screen 19:354–368. https://doi.org/10.1177/1087057113503494

Vranic S, Gosens I, Jacobsen NR, Jensen KA, Bokkers B, Kermanizadeh A, Stone V, Baeza-Squiban A, Cassee FR, Tran L, Boland S (2017) Impact of serum as a dispersion agent for in vitro and in vivo

toxicological assessments of TiO2 nanoparticles. Arch Toxicol 91: 353–363. https://doi.org/10.1007/s00204-016-1673-3

Wan R, Mo Y, Chien S, Li Y, Li Y, Tollerud DJ, Zhang Q (2011) The role of hypoxia inducible factor-1α in the increased MMP-2 and MMP-9 production by human monocytes exposed to nickel nanoparticles. Nanotoxicology 5:568–582. https://doi.org/10.3109/17435390.2010.537791

Wang B, Sun J-Y, Qian S, Liu XY, Zhang SL, Dong SJ, Zha GC (2013) Adhesion of osteoblast-like cell on silicon-doped TiO2 film prepared by cathodic arc deposition. Biotechnol Lett 35:975–982. https://doi.org/10.1007/s10529-013-1155-0

Winn B, Derrick Quarles CJ, Marcus RK, LaBerge M (2011) Nickel ions inhibit α-actin expression and decrease aspect ratio of rat vascular smooth muscle cellsin vitro. Metallomics 3:934–940. https://doi.org/10.1039/C1MT00035G

Wu Y, Kong L (2020) Advance on toxicity of metal nickel nanoparticles. Environ Geochem Health 42:2277–2286. https://doi.org/10.1007/s10653-019-00491-4

Zarei MH, Shirazi SFH, Aghvami M et al (2018) Analysis of cytotoxic effects of nickel on human blood lymphocytes. Toxicol Mech Methods 28:79–86. https://doi.org/10.1080/15376516.2017.1364314

Zhang H, Yang S, Masako N, Lee DJ, Cooper LF, Ko CC (2015) Proliferation of preosteoblasts on TiO2 nanotubes is FAK/RhoA related. RSC Adv 5:38117–38124. https://doi.org/10.1039/C4RA16803H

Zhao X, Toyooka T, Ibuki Y (2017) Silver nanoparticle-induced phosphorylation of histone H3 at serine 10 is due to dynamic changes in actin filaments and the activation of Aurora kinases. Toxicol Lett 276:39–47. https://doi.org/10.1016/j.toxlet.2017.05.009